New Object Based Model for Automatic Building Extraction by Integrating LiDAR Point Clouds and LiDAR Derived Layers

Lamyaa Gamal El-Deen Taha and Rania Elsayed Ibrahim

National Authority for Remote Sensing and Space Sciences

***Abstract*—** Building information is needed for many applications such as updating cadastral databases, management of urban area, building inventory data for damage assessment after disaster and creation of 3D models, building data for solar energy estimation.

Light Detection and Ranging (LiDAR) has become a valuable data source for urban data acquisition.

A method was proposed in this research for building extraction based on object oriented classification with decision rules. A model has been developed using object oriented classification and is implemented using QGIS.

Using Lastools, Envi 5.1 and QGIS 2.10, multiple images were derived from LiDAR data. A total of 30 feature attributes have been generated only 8 of the 30 possible attributes were used, resulted in a classification based on the total group of attributes (raw 3D point clouds data captured by laser scanning and LiDAR-derived features (Digital Surface Model and Digital Terrain Model, textures from Grey Level Co-occurrence Matrix) as well as the area of building≥ a threshold and building shape has been also used. Three classes were identified for the study area: Building, trees and power lines.

The proposed method was evaluated using some buildings of used data set and the results proved high efficiency and reliability of the proposed method for extraction of buildings.

The results show that the proposed method has very high classification accuracy. Particularly, the overall classification accuracy was 92%, and the Kappa coefficient was 0.93. Additionally, both producer accuracy and user accuracy were higher than 86% for buildings class. By counting the extracted buildings in the study area using the model, it was seen that 91% of buildings were extracted automatically.

It was found that a good result could be achieved from the developed method.

***Keywords*—** Building extraction, Object based classifier, LiDAR- 3D Point cloud, Object oriented based classification and Multi-Cue Integration.

Manuscript received November 19, 2015:

TAHA L.G. is with the National Authority for Remote Sensing and Space Sciences, Cairo, Egypt (phone: 202- 26251218; fax: 202-26225800; e-mail: Lamyaa@narss.sci.eg

Ibrahim R.E. ,is with the National Authority for Remote Sensing and Space Sciences, Cairo, Egypt (e-mail: ranyaalsayed@gmail.com, raniaelsayed@narss.sci.eg)

I. Introduction

BUILDING representations are needed in cartographic analysis, urban planning, and visualization [1]. One of the primary tasks in urban remote sensing is to extract building information from various data sources [2]. Building detection and extraction from the measurement data has been a major subject in photogrmmetry and remote sensing [3].

Light Detection and Ranging (LiDAR) is probably the leading technology for the extraction of information about topographic surfaces [4]. The main advantage of LiDAR technique is that it provides dense, discrete, detailed and accurate point coverage over both the objects and surfaces, which has led to an increasing interest in utilizing the data for a range of applications such as mapping, forestry, urban planning, telecommunication and building extraction [5].

LiDAR sensor delivers 3D point clouds with the intensities of the returned signals. In some cases, multiple pulses or full waveform signals can be provided by certain hardware systems [6].

LiDAR technology has received great attention due to its ability to accurately measure the shape and height of objects suitable for a large range of applications such as generating Digital Elevation Models (DEM's) and modelling 3D city environment [7].

LiDAR consists of three main components: (i) GNSS (Global Navigation Satellite System GNSS), (ii) an Inertial Measurement Unit (IMU) and (iii), a Laser Scanner Unit. While the GNSS receiver is used to record the aircraft position, the IMU measures the angular attitude of the aircraft (roll, pitch and yaw or heading). The Laser scanner unit transmits pulses of light toward the surface of interest and records both the travel time of the laser beam and the energy which is reflected by the surface [8] -[10].

LiDAR can collect a georeferenced three dimensional points from both first and last returns. The LiDAR points being on the terrain are separated from points on buildings and other object classes; Digital Surface Model (DSM) and Digital Terrain Model (DTM) can be computed easily and quickly [3] [11].

User should be careful to specify whether first or last return data are required because first return LiDAR data are appropriate for surveying the first reflective surface (tree- tops and rooftops) whereas last return LiDAR data are appropriate for surveying the bare earth terrain, upon completion the post-processing. However, in reality ,last returns are most common[12].

Sensor integration is one of the trends in earth observation and remote sensing. Nowadays main LiDAR vendors are providing integrated laser scanning and imaging sensor systems. Currently the cameras used in the integrated ssystems are usually only used for generating orthophotos [8].

It is very beneficial to recognize a building by combining the complementary properties of laser scanning data and images, such as combining high-resolution satellite images with airborne laser scanner, and fusion of LiDAR data and aerial imagery for classification in order to separate buildings from other categories [3]. A complete set of features can be extracted from the images describing spectral, texture and structural properties of the objects [13]. With the emergence of multi-sensory and laser scans creating point cloud data of higher accuracy and higher point density, digital elevation models such as digital terrain and surface models, provided the additional information, such as shape, texture, and elevation data on the edges, which can be integrated using object-based image processing [14].

Classification means the process to categorize the data into feature classes, such as building, trees and roads [2]. Traditional classification methods are based on pixel based classification. New digital image analysis algorithm, such as that used in object oriented classification, is based on semantic information to interpret an image [15]. Object-based classification can solve the ‘’noise ‘’ in classification caused by the complexity of landscape [16].

The basic idea of object-based classification is to classify not single pixels but groups of pixels that represent already existing objects in a GIS database (or segments) [17] [18].

It analyses the image based on image segments and extract real world objects from those segments. Object- oriented classification contains two main steps which are image segmentation and classification [16].

Before carrying out feature extraction and classification steps, these techniques require image segmentation. Segmentation refers to the process of partitioning a digital image into multiple segments, called image-objects or simply objects, in order to simplify and/or change the representation of an image into a more meaningful and/or homogeneous structure that is easier to understand [13].

Object-based classification can use not only spectral information but also other information such as shape, size, texture, and contextual relationships [17] [19].

Object-oriented image analysis is divided into three steps: Multiresolution segmentation, Create general classes, and Classification rules [20].

There are some techniques for improving the classification accuracy. Using high resolution images for classification; considering of pattern recognition and texture analysis; integration of GIS and remotely sensed data[16].

Object such as building roofs have similar spectral values, which make it difficult to separate them using only spectral information. In addition, even the same objects, can be made of different materials and may be separated into different classes. Therefore, a combination of spatial and textural information and LiDAR-based features can be used in classification in order to improve classification accuracy and building extraction results.

Textures analysis plays an important part in object extraction. Texture analysis takes into consideration of the distribution and variation of neighborhood pixel data. Hence, the spatial properties of land cover classes can be incorporated as one of the classification criterion [21]. From a broad sense, texture can be defined as the visual effect caused by spatial variation in tonal quantity over relatively small areas. It can be used to distinguish between objects which have different spectral information; moreover, it also can tell the difference between objects which have similar spectral characteristics[16] [22].

In this paper, a framework is presented to extract buildings based on a combination of multiple information, such as 3D point cloud, shape, textures from Grey Level Co-occurrence Matrix (GLCM) and area have been used, to achieve more reliable classification as compared to using only a single feature or information. It is an object-oriented method that is based on the buildings’ geometric shape characteristics. Belgium study area was used to assess the performance of the proposed method.

The objectives of this research were :

• To develop a model to identify features from LiDAR derivatives suitable for building extraction based on rules.

• To detect and extract building using object-based classification from raw 3D point cloud data captured by laser scanning and on LiDAR-derived layers (DSM, DTM, textures) as well as the area of building≥ a threshold and Building shape has been also used.

II. Study area and data set

The developed method has been tested on free sample dataset of the Zeebruges, Belgium study area.

The data cover an urban and harbor area in Zeebruges, Belgium, and were acquired and provided for the Contest by the Belgian Royal Military Academy(we use tile 1 only). The imaging data were acquired on March 13, 2011, using an airborne platform flying at the altitude of 300 (m) over the urban and the harbor areas of Zeebruges, Belgium (51.33° N, 3.20° E). The data were collected simultaneously and were georeferenced to WGS-84. The LiDAR data were captured with Riegl laser scanner

LiDAR data at about 10 (cm) point spacing; to avoid leave

cover, the LiDAR data were collected during the spring season. The laser scan rate, angle, and frequency were 125(Hz), 20°, and 49(Hz), respectively. The scanning mode was "last, first and intermediate. The point density for the LiDAR sensor was approximately 65 (points/m²), which is related to point spacing of approximately 10(cm). Both the 3D point clouds(.txt) format and the resulting DSM are provided. Figure 1.a depicts LiDAR DSM

A text file listing the 3D points in XYZI format [containing X (latitude), Y (longitude), Z (elevation), and I (LiDAR intensity) information] was provided.

Color orthophoto at 5(cm) spatial resolution. The color orthophotos were taken at nadir and have a spatial resolution of approximately 5(cm). Figure 1.b depicts color orthophoto at 5(cm) spatial resolution.

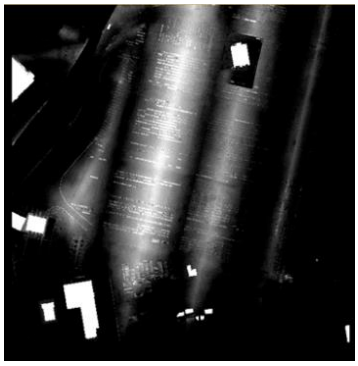

Fig. 1.a LiDAR DSM.

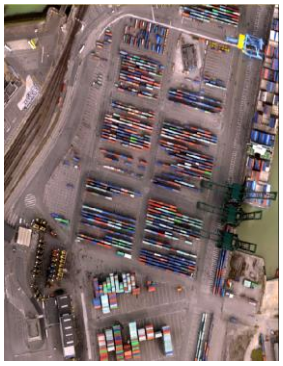

Fig. 1.b Color orthophoto at 5(cm) spatial resolution.

III. Methodology

In this section we describe in details the procedures and the set of rules used by our classification framework.

Object-based classification generally consists of three steps(Fig. 2), including 1) creation of image objects using an image segmentation algorithm, 2) extraction of object-based metrics, and 3) classification using the object-based metrics to extract the building based on combinations of 3D point clouds and LiDAR -derived metrics [17]. Figure 3 show Visualization of 3-D LiDAR las point clouds colored by height using PointVue software.

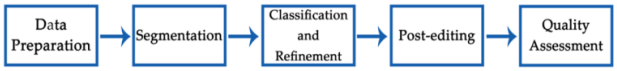

Fig. 2 Object based classification.

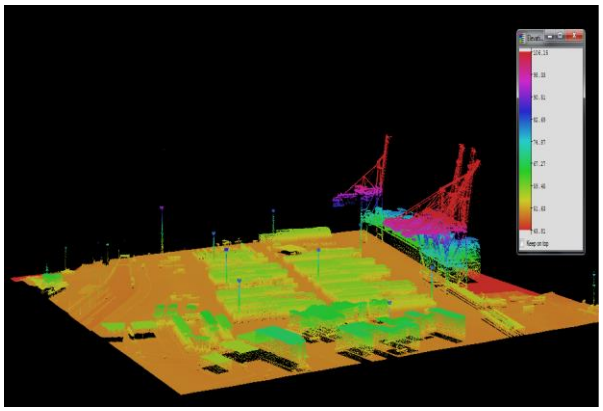

Fig. 3 Visualization of 3-D LIDAR las point clouds colored by height using PointVue software.

The three-stage framework that has been carried out for automatic building extraction based on object oriented classification of an airborne LiDAR data set. In the first stage, pre-processing steps were applied. In the second stage, generate objects using the model. Finally, accuracy assessment steps were performed which include classifications accuracy assessment and assessment of correctness and completeness.

A. Pre-processing

The LiDAR data delivered by the vendor included bare earth elevation points (x, y, z) in txt format. The text file was converted to Las format file using txt2las module in Lastools software package.

Techniques integrating LIDAR data and imagery can be divided into two groups: i) techniques use the LiDAR data as the primary cue for building detection and employ the imagery only to remove vegetation and ii) integration techniques, which use both LiDAR data and imagery as primary cues to delineate building outlines.

The proposed framework belongs to the first group. The first group use the full information of the LiDAR point cloud or interpolate point cloud into a grid format [23]. Density map was generated of the LiDAR raw data to ensure that the results will not contain false readings. Density of 60% of points was 44.62 (Fig. 4) for belgeium area.

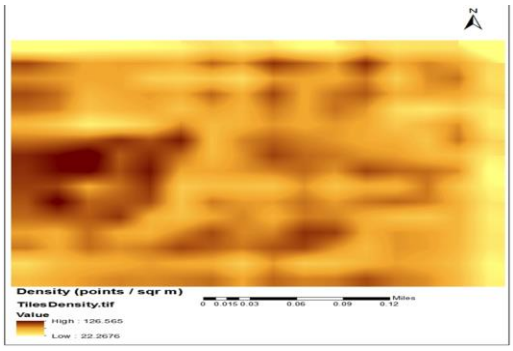

Fig. 4 Density map of Belgeium.

B. *Generate objects using the model*

A model was created using QGIS 2.10 and Envi5.1 for building extraction based on object (rule) based classification, utilizing from the raw 3D point cloud data captured by laser scanning and LiDAR-derived layers. Figure 5 depicts flowchart of developed building extraction model.

The buildings were extracted by an object-oriented method in which the targets are to be analyzed as objects. The single ground object can be generated by grouping neighboring LiDAR points into an object area. The ground points and non-grounds points have been separated after segmentation. To generate single object, we can group adjacent points by means of region growing technique [24] (a region-growing technique to obtain regions with a step edge along their border and a grouping of connected sets of pixels on the basis of an 8-classes partition of the height gradient orientation) .

The first step of the model was segmentation, which divided the image into logical regions or objects with common properties [25]. Segmentation plays an important role for meaningful analysis and correct representation of the objects in the image before classification [14]. A total of 30 feature attributes have been generated only 8 of the 30 possible attributes were used, resulted in a classification based on the total group of attributes (raw 3D point clouds data captured by laser scanning and LiDAR -derived features (DSM, DTM, textures from GLCM) of DSM and DTM) as well as the area of building ≥ a threshold and building shape has been also used. Table 1 shows used rules of buildings extraction. As a result, three land cover classes were identified which are: buildings, trees and power lines.

Table 1 Rules of buildings extraction.

Rules	Value
Shape	Rectangle
Area	>= 10 (sqr m)
Near ground filter width	3 (m)
Buildings Points Range	1.2
Plane Surface Tolerance	0.5 (m)

B.1 Noise Elimination

It is necessary to eliminate the influence of small noise objects, e.g. tree and cars. In the developed model, noise was eliminated according to size threshold.

B.2 Building Extraction

It is important to analyze the buildings' characteristics and to setup the rules for extracting buildings. With the aid of color orthophoto (Fig. 1.b), most buildings have some common characteristics about these buildings objects can be found after analysis.

Firstly, the orthography of a building is made up by some regular rectangles. Secondly, buildings are closed shells that faces possess an orientation and that faces are not allowed to intersect one another. These semantic characteristics determine that the LiDAR points of building objects are distributed in a special form, and on the basis of these characteristics, buildings can be distinguished from trees.

Some geometric conditions of buildings were used to remove the objects of non-buildings such as shape was rectangle. A connected component analysis of the resulting image was applied to obtain the initial building regions. Surfaces with an area less than 10 (m^2) are filtered out before processing continues near ground filter width is set to 3(m) for preventing buses, trucks, train cars, and so forth from being classified as buildings. Buildings points range was set to 1.2 for detecting building planes when the point density is not equal throughout the data. Plane surface tolerance was 0.5(m) this is the allowed vertical tolerance for searching for the surface in the neighboring points. Terrain texture was used for roofs with line width =2.

The explicit height information contained in LiDAR data can also help to distinguish elevated buildings, trees objects from the ground. There are two different kinds of information in LiDAR data: (a) the height of the terrain and (b) The local height of the objects on the terrain. Particularly, the process of classifying a LiDAR dataset into ground (bare-earth) measurements and non-ground measurements is termed as filtering [26].

Textures from GLCM were calculated for DSM, and DTM using ENVI 5.1. Examination of texture measures visually and selection of the best measure for inclusion in the classification experiments.

Four main issues arise in raw data interpolation:

Outlier filtering; A random point is selected as seed point, and to seek adjacent points around the seed point in certain distance, then to shape one region. Table 1 shows used rules of buildings extraction.

The choice of the grid spacing; Ideally, in the context of building reconstruction cell size would be 3 (m).

What kind of interpolation to use when several data points fall into a grid cell. There is a problem that the area of buildings is possibly mixed with vegetation, and the LIDAR points in these areas cannot be separated into two objects easily. Buildings' geometric shape characteristics were used to solve this problem because the two types are significantly different in geometric shape. A rectangular restriction was added to the processing of region growing to be sure that the building and vegetation can be separated successfully. Then geometric and topological relationships among regions resulting from segmentation are computed and stored in a database.

Handling data gaps; With several points in the cell, the median was used unless there is evidence of a step edge; if this was the case, an average that weights more low points in DTM generation and more high points in building extraction was computed.

The method proposed assumed that there are a set of known attributes that can be used to separate the target, or object of

interest. A first important aspect of this method is to combine data classification and building extraction, putting the topological description of the data at the core of both tasks. The rule-based scheme itself represents a second characteristic of our method making it easily adaptable to different situations. A third important characteristic of our method is that it uses grid data to take advantage of their regularity in data processing. The hierarchical structure of the method enables reasoning about data relationships at an appropriate scale and provides the contextual information essential to increase the probability of correct classification of each data point in the final stage. A disadvantage is that it discards information that may still be of use.

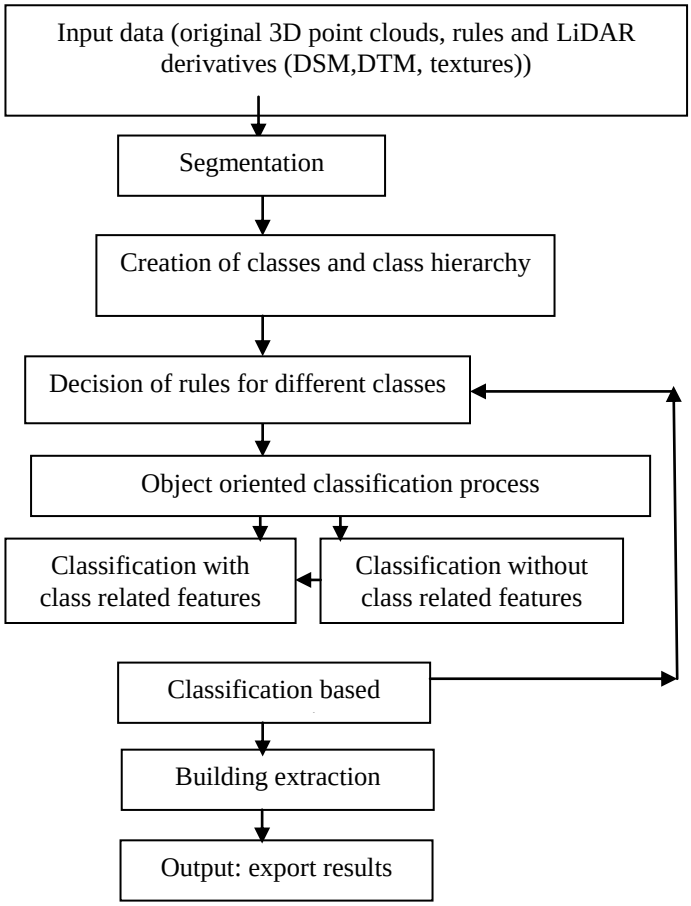

Fig. 5 Flowchart of the model.

C. Creation of LIDAR DTM

DTM was generated using Lastools. Figure 6.a illustrates LIDAR DTM. Figure 6.b illustrates overlay of LIDAR DSM& DTM (coregistration). Figure 6.c illustrates DSM visualization from the proposed method.

Using the difference between a (1) DSM and (2) DTM, a normalized DSM (nDSM) can be produced. Objects that are less than 3(m) were removed to minimize features that have similar geometry as that of buildings.

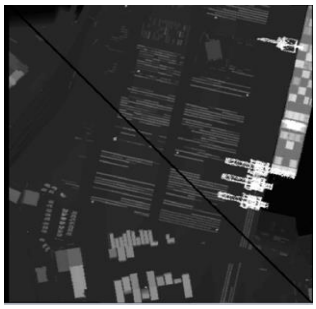

Fig. 6.a LiDAR DTM

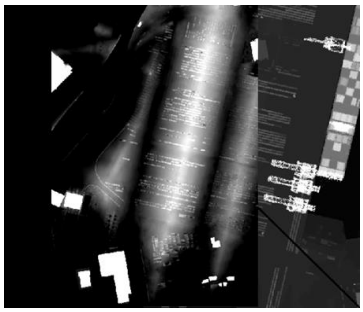

Fig. 6.b Overlay of DSM& DTM (coregistration)

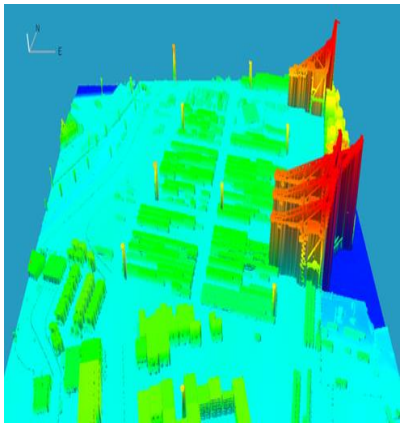

Fig. 6.c Visualization of 3-D LIDAR las point clouds colored by height using developed model

D. Creation of Textures

Different land use classes cannot be distinguished only by their spectral behavior but also because of different textures[18]. The window size for texture analysis should be smaller than the smallest object to be mapped in the image[21]. In our method, eight textures attributes were used based on GLCM with a window size 3 * 3 (Contrast, Dissimilarity, Homogeneity, Entropy, Mean,Variance, Correlation, Angular Second Moment).

Textures from GLCM were calculated for DSM and DTM using ENVI 5.1 (total of 16 Texture features). The texture measures were visually examined and the best measure was chosen for inclusion in the classification experiments. Table 2. show visual analysis (interpretability) of different texture measures.

$$\text{Mean} = \sum_{x=0}^{N-1} \sum_{y=0}^{N-1} x P_{x,y} \qquad (1)$$

where P is the normalized symmetric GLCM of dimension $G \times G$, G is the number of grey levels and $P_{x,y}$ is the element of P in the x^{th} row and the y^{th} column [21].

N-1 N-1

$$\text{Contrast=Con}=\sum_{x=0}^{} \sum_{y=0}^{} P_{x,y}(x-y)^2 \quad (2)$$

$$\text{Correlation=Cor}=\sum_{x=0}^{N-1} \sum_{y=0}^{N-1} P_{x,y}\,(x-\mu x)\,(y-\mu y)/\sigma x\,\sigma y \quad (3)$$

σx and σy are the standard deviation of row x and column y

μ x and μ y are the mean of row x and column y

$$\text{Entropy=Ent}=\sum_{i=0}^{N-1} \sum_{j=0}^{N-1} P_{i,j}\,(-\ln P_{i,j}) \quad (4)$$

$$\text{Homogeneity = Hom}=\sum_{i=0}^{N-1} \sum_{j=0}^{N-1} P_{i,j} / 1+(i-j)^2 \quad (5)$$

$$\text{Dissimilarity=Dis} = \sum_{i=0}^{N-1} \sum_{j=0}^{N-1} P_{i,j} \mid i-j \mid \quad (6)$$

$$\text{Angular Second Moment= ASM}=\sum_{i=0}^{N-1} \sum_{j=0}^{N-1} P^2_{i,j} \quad (7)$$

[16][25].

Table 2. Visual analysis (interpretability) of different texture measures.

Texture measure / Feature	Mean	Var	Hom	Con	Dis	Ent	ASM	Cor
Buildings from DSM	√√√√	√√	√√	√	√	√√√	√√	√
Buildings from DTM	√√√√	√√	√√	√	√	√√√	√√	√

√√√√ :high √√√:medium √√:low √: very low

From the visual analysis it was found that the best separation building class results using mean texture measure(mean texture measure of DSM and mean texture measure of DTM). This followed by entropy measure. Figure 7.a illustrates mean texture measure of DSM. Figure 7.b illustrates mean texture measure of DTM.

Fig7.a Mean of DSM.

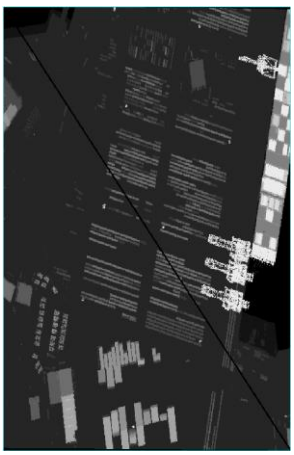

Fig7.b Mean of DTM.

D. Output

As a result of running the model for object based classification, shapefile of buildings and an output table containing the area of buildings, perimeter, height. Figure 8.a depicts extracted buildings. Figure 8.b depicts buildings attributes.

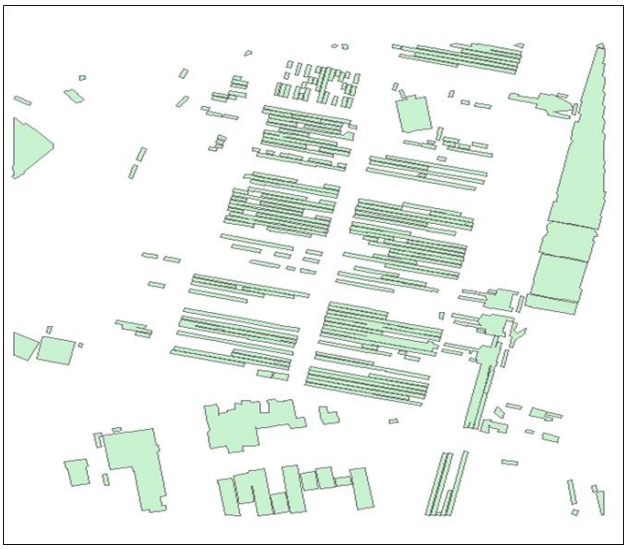

Fig. 8.a Extracted buildings from the proposed method.

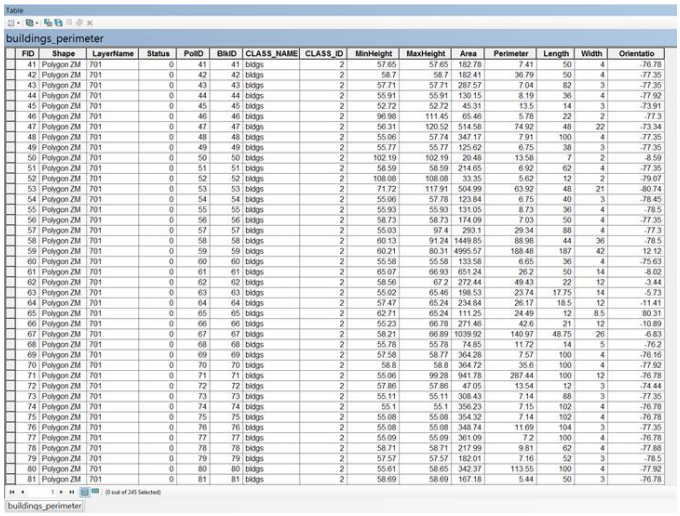

buildings_perimeter

FID	Shape	LayerName	Status	PolID	BlkID	CLASS_NAME	CLASS_ID	MinHeight	MaxHeight	Area	Perimeter	Length	Width	Orientatio
41	Polygon ZM	701	0	41	41	bldgs	2	57.65	57.65	182.78	7.41	50	4	-76.78
42	Polygon ZM	701	0	42	42	bldgs	2	58.7	58.7	182.41	36.79	50	4	-77.35
43	Polygon ZM	701	0	43	43	bldgs	2	57.71	57.71	287.57	7.04	82	3	-77.35
44	Polygon ZM	701	0	44	44	bldgs	2	55.91	55.91	130.15	8.19	36	4	-77.92
45	Polygon ZM	701	0	45	45	bldgs	2	52.72	52.72	45.31	13.5	14	3	-73.91
46	Polygon ZM	701	0	46	46	bldgs	2	96.98	111.45	65.46	5.78	22	2	-77.3
47	Polygon ZM	701	0	47	47	bldgs	2	56.31	120.52	514.58	74.92	48	22	-73.34
48	Polygon ZM	701	0	48	48	bldgs	2	55.06	57.74	347.17	7.91	100	4	-77.35
49	Polygon ZM	701	0	49	49	bldgs	2	55.77	55.77	125.62	6.75	38	3	-77.35
50	Polygon ZM	701	0	50	50	bldgs	2	102.19	102.19	29.48	13.58	7	2	-8.59
51	Polygon ZM	701	0	51	51	bldgs	2	58.59	58.59	214.65	6.92	62	4	-77.35
52	Polygon ZM	701	0	52	52	bldgs	2	108.08	108.08	33.35	5.62	12	2	-79.07
53	Polygon ZM	701	0	53	53	bldgs	2	71.72	117.91	504.99	63.92	48	21	-80.74
54	Polygon ZM	701	0	54	54	bldgs	2	55.06	57.78	123.84	6.75	40	3	-78.45
55	Polygon ZM	701	0	55	55	bldgs	2	55.93	55.93	131.05	8.73	36	4	-78.5
56	Polygon ZM	701	0	56	56	bldgs	2	58.73	58.73	174.09	7.03	50	4	-77.35
57	Polygon ZM	701	0	57	57	bldgs	2	55.03	97.4	293.1	29.34	88	4	-77.3
58	Polygon ZM	701	0	58	58	bldgs	2	60.13	91.24	1449.85	88.98	44	36	-78.5
59	Polygon ZM	701	0	59	59	bldgs	2	60.21	80.31	4995.57	188.48	187	42	12.12
60	Polygon ZM	701	0	60	60	bldgs	2	55.58	55.58	133.58	6.65	36	4	-75.63
61	Polygon ZM	701	0	61	61	bldgs	2	65.67	66.93	651.24	26.2	50	14	-8.02
62	Polygon ZM	701	0	62	62	bldgs	2	58.56	67.2	272.44	49.43	22	12	-3.44
63	Polygon ZM	701	0	63	63	bldgs	2	55.02	65.46	198.53	23.74	17.75	14	-5.73
64	Polygon ZM	701	0	64	64	bldgs	2	57.47	65.24	234.84	26.17	18.5	12	-11.41
65	Polygon ZM	701	0	65	65	bldgs	2	62.71	65.24	111.25	24.49	12	8.5	80.31
66	Polygon ZM	701	0	66	66	bldgs	2	55.23	66.78	271.46	42.6	21	12	-10.89
67	Polygon ZM	701	0	67	67	bldgs	2	58.21	66.89	1039.92	140.97	48.75	26	-6.83
68	Polygon ZM	701	0	68	68	bldgs	2	55.78	55.78	74.85	11.72	14	5	-76.2
69	Polygon ZM	701	0	69	69	bldgs	2	57.58	58.77	364.28	7.57	100	4	-76.16
70	Polygon ZM	701	0	70	70	bldgs	2	58.8	58.8	364.72	35.6	100	4	-77.92
71	Polygon ZM	701	0	71	71	bldgs	2	55.06	99.28	941.78	267.44	100	12	-76.78
72	Polygon ZM	701	0	72	72	bldgs	2	57.86	57.86	47.05	13.54	12	3	-74.44
73	Polygon ZM	701	0	73	73	bldgs	2	55.11	55.11	308.43	7.14	88	3	-77.35
74	Polygon ZM	701	0	74	74	bldgs	2	55.1	55.1	356.23	7.15	102	4	-76.78
75	Polygon ZM	701	0	75	75	bldgs	2	55.08	55.08	354.32	7.14	102	4	-76.78
76	Polygon ZM	701	0	76	76	bldgs	2	55.08	55.08	348.74	11.69	104	3	-77.35
77	Polygon ZM	701	0	77	77	bldgs	2	55.09	55.09	361.09	7.2	100	4	-76.78
78	Polygon ZM	701	0	78	78	bldgs	2	58.71	58.71	217.99	9.81	62	4	-77.88
79	Polygon ZM	701	0	79	79	bldgs	2	57.57	57.57	182.01	7.16	52	3	-78.5
80	Polygon ZM	701	0	80	80	bldgs	2	55.61	58.65	342.37	113.55	100	4	-77.92
81	Polygon ZM	701	0	81	81	bldgs	2	58.69	58.69	167.18	5.44	50	3	-76.78

(0 out of 245 Selected)

buildings_perimeter

Fig. 8. b Buildings attributes

E. Classifications accuracy assessment

Classification assessment was based on the analysis of the confusion matrix, by comparing the class assigned to each evaluation sample with the reference information. Accuracy assessment was conducted with QGIS 2.10 for each of the resulted classifications with reporting of a series of performance metrics including producer's and user's accuracies, overall accuracy, and Kappa Coefficient of agreement. Table 3 show accuracy results from object-based classification. Producer's and user's accuracies for the building class were equal 86% and 89% respectively.

The performance of a maximum likelihood supervised classifier (MLH) was used to compare to the developed model.

The maximum likelihood supervised classification was conducted using three land-cover classes (buildings, tree and power line). Firstly training data was selected for the three classes and evaluated. The outcome of a maximum likelihood classifier was used as a performance measure. The detailed comparison results are listed in Table 3.

Table 3 Accuracy results from object-based classification compared to maximum likelihood classifier.

Class Name	Overall accuracy %	Buildings Producer's accuracy %	Buildings User's accuracy %	Kappa Statistic
Object-based classification	92	86	89	0.93
Maximum likelihood	89	82.30	86.10	0.90

F. Comparison of Object-based feature extraction results with reference vector

Conventional manual feature extraction is a time consuming and low efficiency. By overlaying the reconstructed roof planes and reference data, the overlapped area of them is calculated. If the ratio of this overlapped area to area of the reconstructed roof plane is larger than 80%, the reconstructed roof plane is taken as true one. Otherwise, it is considered as a wrong one. If a roof plane is not be detected by the automatic process, we call it a mis-detected roof plane [28].

The roof planes derived by manually digitizing of color orthophoto using ArcGIS 10.1 were taken as reference data.

Vector results of object-based feature extraction of buildings were compared and superimposed with reference vectors. By counting the extracted buildings in the study area using the model, it was seen that 91% of buildings were extracted automatically. The extracted buildings were good shaped and similar to their real forms.

G. Overlaying and color orthophoto

By overlaying the extracted building roofs and color orthophoto. It was found that Overall, the results were satisfactory. Figure 9 illustrates overlay of extracted building

Fig. 9 Overlay of extracted building roofs over color orthophoto.

H. Assessment of correctness and completeness

The focus of this analysis was to estimate the correctness and completeness of the reconstructed roof planes in these3D models. The correctness and completeness of 3D roof plane were calculated according to [16]

Completeness=TP/TP+FN (9)

Correctness= TP/TP+FP (10)

Branching Factor (BF) = FP / TP (11)

Miss Factor= FN / TP (12)

Building Detection Percentage(DP) : 100 * TP / (TP+ FN) (13)

Quality Percentage: 100 * TP / (TP + FP + FN) (14)

where;

TP (true Positive) is the number of true roof planes (both reference data and extracted result are buildings).

TN(true Negative) both reference data and extracted result are background.

FP (false Positive) is the number of wrong roof planes

(extracted result is building but reference data is not building).

FN (false Negative) is the number of mis-detected roof planes(reference data is building but extracted result is not building).

The 'branching factor' indicates the rate of incorrectly labelled building areas, while the 'miss factor' describes the rate of missed building areas. The branching factor increases when the algorithm over-classifies height measurements as those of buildings, while the miss factor increases when the algorithm misses buildings [14]. The 'building detection percentage' gives the percentage of building areas correctly extracted by the automatic process and the 'quality percentage' is the overall measure of performance which accounts for all misclassifications and describes how likely a building area produced by the automatic extraction is true [29][30].

Three building blocks of different sizes and shapes have been chosen for testing the quality of the proposed approach see table 4

Table 4 Quality assessment of the results of building extraction from the developed model.

Quality assessment	Building block1	Building block2	Building block3
FP	0	0	0
FN	5	0	2
TP	18	4	15
MF	0.277	0	0.133
BF	0	0	0
DP	78.26	100	88.24
QP	78.26	100	88.24
Completeness	0.7826	1	0.882
Correctness	1	1	1

Areas of some buildings with different shapes have computed. Table 5 indicates areas of some buildings resulted from the object based model to areas from MLH.

Table 5 Areas of some buildings resulted from the object based model compared to areas from MLH.

Area(m2)	Manual	Maximum likelihood	Developed model
Building1	287.83	286.93	287.57
Building2	199.03	197.56	198.53
Building3	308.25	306.91	308.43
Building4	218.06	211.56	217.99

IV. Results and Discussion

A method was proposed in this research for building extraction based on object oriented classification with decision rules. A model has been developed using object oriented classification and was implemented using QGIS 2.10 and Envi 5.1 resulted in a classification based on the raw 3D point cloud data captured by laser scanning and LIDAR-derived features (DSM,DTM, textures from GLCM) as well as the area of building≥ a threshold and building shape has been also used.

An important point both for higher success rate but also lower processing costs is the number and type of used cues for object extraction.

An increased number of cues are derived from the LIDAR data, LiDAR derivative layers were generated using LAStools and are combined; correct cue combination and uncertainty propagation largely remains an unsolved problem. A total of 30 feature attributes have been generated only 8 of the 30 possible attributes were used, resulted in a classification based on the total group of attributes (raw 3D point clouds data captured by laser scanning and LIDAR-derived features (DSM,DTM, textures from GLCM of DSM and DTM)) as well as the area of building≥ a threshold and building shape has been also used.

Since building roofs are located very close one another with simple shapes and different colors, the extraction of building outlines was easy by object-based classification and even by manual interpretation.

The sizes of buildings vary greatly while most of the shapes of building roofs are rectangular.

Buildings with uniform roof-color were classified correctly. However, some buildings were misclassified and classified as building blocks. The failures in building detection were caused by the lower elevation of buildings, buildings mix with trees and the unsuccessful closing operator. The buildings would be removed while the difference of buildings and grounds is smaller than a threshold. Besides, the buildings which mix with trees would be retained since the roughness value is smaller than a threshold and could not be removed by the texture. The unsuccessful closing operator would cause the initial building searching to fail. Also the materials of building roofs are also different

The performance of a maximum likelihood supervised classifier was used to compare the building detection and extraction from the developed model.

The overall accuracy of the maximum likelihood classifier was 89% and the Kappa coefficient was 0.90.

The statistics in Table 3 show that our proposed method has very high classification accuracy. Particularly, the overall classification accuracy is 92%, and the Kappa coefficient is 0.93. Additionally, both produce accuracy and user accuracy higher than 86% for building class.

By counting the extracted buildings in the study area using the model, it was seen that 91% of buildings were extracted automatically.

Based on Table 4, it is clear that a higher DP together with a low BF which indicates a good performance.

By comparing the areas of some buildings resulted from the model and the results from manual extraction and maximum likelihood classifier results, based on Table 5, it is clear that the model has a better accuracy than the maximum likelihood classifier in area computation.

V. Conclusions and Further work

Building extraction becomes one of important fields of research in photogrammetric and machine vision.

New automatic building detection and extraction model based on object-based classification was developed and implemented using QGIS 2.10 and Envi5.1.

Building extraction data are necessary in many applications. In this study, the capacity of object-based classification approach to identify buildings was examined.

An object-based analysis method was proposed to classify multi cue(the raw 3D point clouds in urban areas as well as LIDAR-derived features (DSM, DTM, textures from GLCM).

A first important aspect of developed method is combining data classification and building extraction, putting the topological description of the data at the core of both tasks. The rule-based scheme itself represents a second characteristic of our method making it easily adaptable to different situations. A third important characteristic of our method is that it uses grid data to take advantage of their regularity in data processing. The hierarchical structure of the method enables reasoning about data relationships at an appropriate scale and provides the contextual information essential to increase the probability of correct classification of each data point in the final stage. A disadvantage is that it discards information that may still be of use.

It was found that manual on-screen digitizing method process is slower than the automatic one but it has more close results as the real feature forms. The object based classification yields a higher accuracy than maximum likelihood supervised classification with an overall accuracy of the rule classifier is 92%, and the Kappa coefficient is 0.93.

Under the object- based approach, both user and producer accuracies for the building class were higher than obtained using pixel based method (maximum likelihood supervised classifier). Our method relies on a very simple but effective segmentation, which allows the straightforward the discrimination between of most vegetation and buildings from the terrain

A higher DP together with a low BF indicates a good performance. The main innovation of the proposed method is the classification was made in segment-wise style rather than point-wise one.

It was found that the proposed method is more effective than maximum likelihood method. Also Object-oriented classification is also more robust to noise compared to pixel-based classification of buildings.

Further work is planned concerning processing of point cloud and imagery simultaneously. Reconstructed shape of the building will be also the topic of further research.

Acknowledgment

The authors thank The 2015 IEEE GRSS Data Fusion Contest for giving us the data. The editing and comments of the reviewers are gratefully appreciated.

References

[1] N. M. Farhad and S. Zadegan, "Segmentation of LIDAR DATA for extracting building's roof shapes, using fuzzy logic concepts, GIS Ostrava," in *Proc. Surface models for geosciences Conf., Ostrava January 23. – 25., 2012.*

[2] j. Shan and A. Sampath, '' Urban terrain and building extraction from airborne LIDAR data. In *''Urban remote sensing,* Weng, Ed. Q…. CRC press: Taylor & Francis, 2007.

[3] C. K. Wang, and P.H. Hsu, '' Building detection and structure line extraction from airborne LIDAR DATA,'' *The International Archives of the Photogrammetry, Remote Sensing and Spatial Information Sciences.* vol. XXXVII, Part B3b, 2008.

[4] M. Salah and J. Trinder '' Support vector machines based filtering of LiDAR Data: A Grid Based Method,'' in *Proc. FIG Congress, Sydney, Australia, 2010, pp.11-16.*

[5] J. Shen, J. Liu, X. Lin, and R. Zhao ''Object-Based Classification of Airborne Light Detection and Ranging Point Clouds in Quatt Settlements,'' *SENSOR LETTERS,* vol. 10, pp. 1–9, 2012.

[6] J. Zhang "Multi-source remote sensing data fusion: status and trends" *International Journal of Image and Data Fusion.*

[7] J J. Li, Y. Li and M. A. Chapman, ''Building edge extraction from LiDAR based on jump detection in non-parameter regression model," in Proc. 2005. Available:''www.isprs.org/proceedings/XXXVI/5-C55/papers/jun_li.pdf

[8] X. Hu, Z. Zhang, Y. Duan, Y. Zhang, J. Zhu, and H. Long "LIDAR photogrammetry and its data organization" International Archives of the Photogrammetry, Remote Sensing and Spatial Information Sciences, vol. XXXVIII-5/W12, 2011 [Workshop, Calgary, Canada, 2011].

[9] A. Jochem, B. Hofle, M. Rutzinger and N. Pfeifer,2009 "Automatic roof plane detection and analysis in airborne LiDAR point clouds for solar potential assessment," *Sensors*, vol. 9, pp. 5241-5262, 2009.

[10] M. Zhou , B. Xia, G. Sua, L. Tang, and C. Lia ''Study on the target feature extraction from LiDAR point clouds,'' *The International Archives of the Photogrammetry, Remote Sensing and Spatial Information Sciences*. vol. XXXVII. part B3b. 2008.

[11] F. Rottensteiner, and C. Briese "A new method for building extraction in urban areas from high-resolution LIDAR data" Commission III, WG III/3 ISPRS 2002
http://www.isprs.org/commission3/proceedings02/papers/ paper082.pdf

[12] D. Maune, *Digital elevation model technologies and applications the DEM user's manual, 2001.*

[13] L.A. Ruiz , J.A. Recio, A. Fernández-Sarría and T. A Hermosilla " tool for object descriptive feature extraction: application to image classification and map updating" The International Archives of the Photogrammetry, Remote Sensing and Spatial Information Sciences, vol. XXXVIII-4/C7, 2010.

[14] E. R. Lopez, H. F. Santos, R. R. C. S. Ana1, and S. J. D. Samalburo ''Evaluation of building footprint generation from LIDAR data and orthoimages using object-based image analysis technique,'' in *Proc.* ACRS, Philippines, 2015.

[15] A. J. Moreno and J.E. Larriva, ''Comparison between new digital image classification methods and traditional methods for land cover mapping'' in Remote sensing of land use and Land cover, Giri C.P. Ed., CRC press, Taylor & Francis, 2012.

[16] Y. Du "Verification of Tsunami reconstruction projects by object – oriented building extraction from high resolution satellite imagery" M.S. Thesis, international institute of Geo-information science and earth observation, The Netherlands, 2008.

[17] Y. Ke, L. J. Quackenbush and J. Im "Synergistic use of QuickBird multispectral imagery and LIDAR data for object-based forest species classification" *Remote Sensing of Environment*, vol. 114, pp. 1141–1154, 2010.

[18] V. Walter , ''Object-based evaluation of LIDAR and multispectral data for matic change detection in GIS databases''2004. Available: www.isprs.org/proceedings/XXXV/congress/comm2/papers/222.pdf ·

[19] D. M. Styers, L. M. Moskal, J.J. Richardson and M. A. Halabisky ''Evaluation of the contribution of LiDAR data and postclassification procedures to object-based classification accuracy,'' *Journal of Applied Remote Sensing*, vol. 8, 2014.

[20] R. Parivallal, B. L. Dhivya, K. Elango, T. Karthik and B. Nagarajan ''An approach to classify the object from the satellite image using image analysis tool'' *International Journal for Innovative Research in Science & Technology*, vol. 1, Issue 4, pp. 2349-6010, 2014.

[21] A. Shaker, W. Y. Yan, and N. El-Ashmawy ''Panchromatic satellite image classification for flood hazard Assessment'' *Journal of Applied Research and Technology*, vol. 10, pp. 902-911, 2012.

[22] L. Wang, W. P. Sousa, P. Gong and G. S. Biging " Comparison of IKONOS and QuickBird images for mapping mangrove species on the Caribbean Coast of Panama," *Remote Sensing of Environment*, vol. 91, pp. 432–440, 2004.

[23] D. Grigillo and U. Kanjir'' Urban object extraction from digital surface model and digital aerial images,'' ISPRS Annals of the Photogrammetry, Remote Sensing and Spatial Information Sciences, vol. I-3, 2012[XXII ISPRS Congress, August, 25 to September, 2012, Melbourne, Australia]

[24] G. Forlani, C. Nardinocchi , M. Scaioni, and P. Zingaretti "Complete classification of raw LIDAR data and 3D reconstruction of buildings", *Pattern Anal Applic*, vol. 8, pp. 357–374, 2006.

[25] I. M. H. Escamos, A. R. C. Roberto, E. R. Abucay, G.K. L. Inciong, M. D. Queliste, and J.A. C. Hermocilla ''Comparison of different machine learning classifiers for building extraction in LIDAR-derived datasets,''ACRS, Philippines, 2015.

[26] J. X. Zhang and X. G. Lin ''Object-based classification of urban airborne LIDAR point clouds with multiple echoes using SVM,'' *ISPRS Annals of the Photogrammetry, Remote Sensing and Spatial Information Sciences*, vol. I-3, 2012 *[*XXII ISPRS Congress, 25 August – 01 September 2012, Melbourne, Australia]

[27] D. Lu and Q. Weng "Urban Classification Using Full Spectral Information of Landsat ETM_ Imagery in Marion County, Indiana" *Photogrammetric Engineering & Remote Sensing* vol. 71, No. 11, pp. 1275–1284, 2005.

[28] L. Cheng, L. Tong, Y. Chen, W. Zhang, J. Shan, Y. Liu, and M. Li, "Integration of LIDAR data and optical multi-view images for 3D reconstruction of building roofs" *Optics and Lasers in Engineering*, vol.5, pp. 493–502, 2013.

[29] K.D. San and M. Turker "Automatic building extraction from high resolution stereo satellite images "in Proc. Commission VII ISPRS 2007. Available: http://www.isprs2007ist.itu.edu.tr/39.pdf

[30] Z. Lari, and H. Ebadi "Automatic Extraction of Building Features From High Resolution Satellite Images Using Artificial Neural Networks" Commission VII, WG WG VII/2& VII/7 ISPRS 2007. Available: www.isprs2007ist.itu.edu.tr/25.pdf